Subclade of Flavin-Monooxygenases Involved in Aliphatic Glucosinolate Biosynthesis[1][W]

Jing Li[2], Bjarne Gram Hansen[2,3], James A. Ober, Daniel J. Kliebenstein, and Barbara Ann Halkier*

Plant Biochemistry Laboratory, Department of Plant Biology and Villum Kann Rasmussen Research Centre for Pro-Active Plants, Faculty of Life Sciences, University of Copenhagen, DK–1871 Frederiksberg C, Denmark (J.L., B.G.H., B.A.H.); and Department of Plant Sciences, University of California, Davis, California 95616–8780 (J.A.O., D.J.K.)

Glucosinolates (GSLs) are amino acid-derived secondary metabolites with diverse biological activities dependent on chemical modifications of the side chain. We previously identified the flavin-monooxygenase $FMO_{GS\text{-}OX1}$ as an enzyme in the biosynthesis of aliphatic GSLs in Arabidopsis (*Arabidopsis thaliana*) that catalyzes the *S*-oxygenation of methylthioalkyl to methylsulfinylalkyl GSLs. Here, we report the fine mapping of a quantitative trait locus for the *S*-oxygenating activity in Arabidopsis. In this region, there are three *FMO*s that, together with $FMO_{GS\text{-}OX1}$ and a fifth *FMO*, form what appears to be a crucifer-specific subclade. We report the identification of these four uncharacterized *FMO*s, designated $FMO_{GS\text{-}OX2}$ to $FMO_{GS\text{-}OX5}$. Biochemical characterization of the recombinant protein combined with the analysis of GSL content in knockout mutants and overexpression lines show that $FMO_{GS\text{-}OX2}$, $FMO_{GS\text{-}OX3}$, and $FMO_{GS\text{-}OX4}$ have broad substrate specificity and catalyze the conversion from methylthioalkyl GSL to the corresponding methylsulfinylalkyl GSL independent of chain length. In contrast, $FMO_{GS\text{-}OX5}$ shows substrate specificity toward the long-chain 8-methylthiooctyl GSL. Identification of the $FMO_{GS\text{-}OX}$ subclade will generate better understanding of the evolution of biosynthetic activities and specificities in secondary metabolism and provides an important tool for breeding plants with improved cancer prevention characteristics as provided by the methylsulfinylalkyl GSL.

Glucosinolates (GSLs) are amino acid-derived secondary metabolites present in the order Brassicales. Upon disruption of plant tissue by, for example, wounding or mastication, GSLs are hydrolyzed by the thioglucosidases, myrosinases, which produce a range of breakdown products, primarily isothiocyanates and nitriles, with diverse biological activities (Halkier and Gershenzon, 2006; Zhang et al., 2006b). GSLs (typically their hydrolysis products) act as antimicrobials against pathogens, feeding deterrents toward generalist herbivores, and as attractants for specialist herbivores (Kliebenstein et al., 2001a; Tierens et al., 2001). For humans, the well-studied sulforaphane, which is derived from 4-methylsulfinylbutyl (4-MSB) GSL and the isothiocyanates derived from 7-methylsulfinylheptyl (7-MSH) GSL and 8-methylsulfinyloctyl (8-MSO) GSL, are considered very potent cancer-preventive agents because of their strong induction of xenobiotic phase II detoxification enzymes in animals (Zhang et al., 1992; Rose et al., 2000). These isothiocyanates can decrease the risk of developing different cancers, such as breast cancer (Rose et al., 2005), gastric cancer (Fahey et al., 2002), and skin cancer (Talalay et al., 2007). The potent cancer-preventive property of the hydrolysis product of methylsulfinylalkyl (MS) GSLs makes it desirable to characterize the genes that encode for the enzymes that catalyze the *S*-oxygenation reaction from methylthioalkyl (MT) to MS GSLs.

Biosynthesis of MS GSLs can be divided into three separate phases (i.e. Met chain elongation, GSL core structure formation [Halkier and Gershenzon 2006], and, finally, an *S*-oxygenating reaction [Fig. 1]). An Arabidopsis (*Arabidopsis thaliana*) flavin-monooxygenase $FMO_{GS\text{-}OX1}$ was recently shown to catalyze the *S*-oxygenation of MT to MS GSLs (Hansen et al., 2007). The presence of MS GSLs in $FMO_{GS\text{-}OX1}$ T-DNA knockout mutants indicated that additional genes catalyzing this reaction are present (Hansen et al., 2007).

The conversion of MT to MS GSLs was originally studied via genetic means using natural variation in Arabidopsis and *Brassica napus* as defined by the GSL *S*-oxygenation (*GS-OX*) quantitative trait loci (QTLs; Giamoustaris and Mithen, 1996; Kliebenstein et al., 2001a, 2001b, 2002). These studies identified several independent *GS-OX* loci that mapped near $FMO_{GS\text{-}OX1}$, although they did not overlap with the physical position of $FMO_{GS\text{-}OX1}$. These *GS-OX* loci even showed

[1] This work was supported by the Villum Kann Rasmussen (VKR) Foundation (grant to VKR Research Centre for Pro-Active Plants); the National Science Foundation (grant nos. DBI–0642481 and MCB–0323759 to D.J.K.); Research School for Biotechnology graduate school (Ph.D. stipend to B.G.H.); and a Marie Curie IIF fellowship (contract no. MIF1–CT–2006–022344 to J.L.).

[2] These authors contributed equally to the article.

[3] Present address: Center for Microbial Biotechnology, Department of Systems Biology, Technical University of Denmark, DK–2800 Kgs. Lyngby, Denmark.

* Corresponding author; e-mail bah@life.ku.dk.

The author responsible for distribution of materials integral to the findings presented in this article in accordance with the policy described in the Instructions for Authors (www.plantphysiol.org) is: Barbara Ann Halkier (bah@life.ku.dk).

[W] The online version of this article contains Web-only data.
www.plantphysiol.org/cgi/doi/10.1104/pp.108.125757

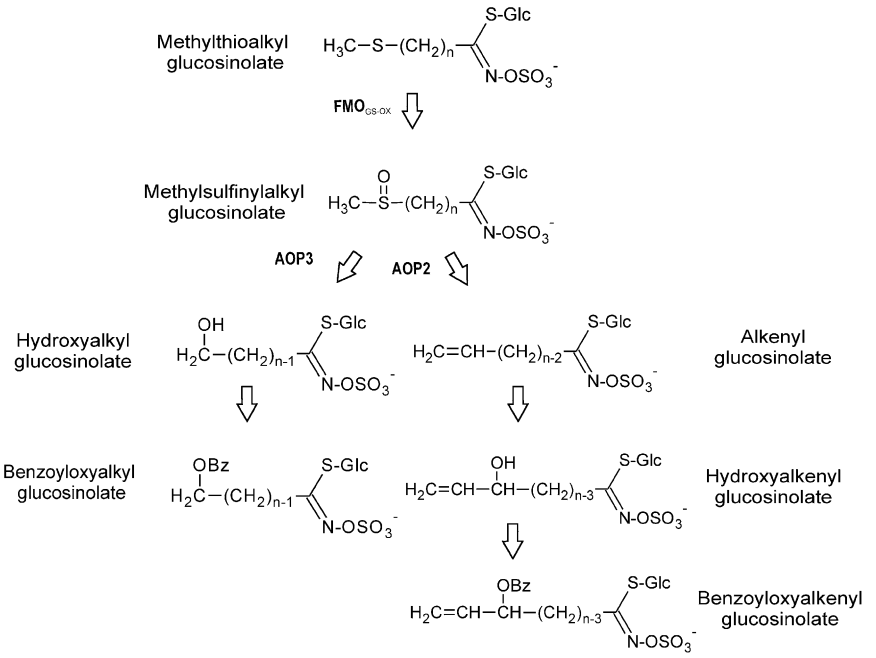

Figure 1. Potential secondary modifications of Met-derived GSLs in Arabidopsis. AOP2 and AOP3, 2-oxoglutarate-dependent dioxygenase. For MT and MS, $n = 3$ to 8. For OH and benzoyloxyalkyl, $n = 2$ to 3. For alkenyl, $n = 2$ to 5. For hydroxyalkenyl and benzoyloxyalkenyl, $n = 3$.

structural specificity such that some affected all aliphatic GSLs, whereas others were specific to subsets of substrates. The QTL study suggests that the *GS-OX* loci near the physical position of $FMO_{GS\text{-}OX1}$ may contain the candidate genes for the additional MT to MS *S*-oxygenating enzyme activity previously suggested (Hansen et al., 2007).

In this article, we identify four $FMO_{GS\text{-}OX1}$-related genes encoding for enzymes that catalyze the MT to MS *S*-oxygenation reaction. By fine genetic mapping analysis, we found that three $FMO_{GS\text{-}OX1}$ homologs, *At1g62540*, *At1g62570*, and *At1g62560*, mapped to a 0.2-Mb area containing a *GS-OX* QTL in multiple Arabidopsis populations. The five *FMO* genes *At1g65860* ($FMO_{GS\text{-}OX1}$), *At1g62540* ($FMO_{GS\text{-}OX2}$), *At1g62560* ($FMO_{GS\text{-}OX3}$), *At1g62570* ($FMO_{GS\text{-}OX4}$), and *At1g12140* ($FMO_{GS\text{-}OX5}$) were found within a subclade of the FMO phylogeny that (at least presently) consists of genes from only cruciferous species. Furthermore, we characterize the Arabidopsis enzymes in this subclade and show that $FMO_{GS\text{-}OX2}$ to $FMO_{GS\text{-}OX4}$ are able to catalyze the *S*-oxygenation independent of chain length, as was observed for $FMO_{GS\text{-}OX1}$, and that $FMO_{GS\text{-}OX5}$ is specific for 8-methylthiooctyl (8-MTO) GSL.

RESULTS

Phylogenetic Tree of Plant FMOs in Proposed Clade III

Previous phylogenetic analysis had shown three plant *FMO* clades from the genomic sequence of rice (*Oryza sativa*), Arabidopsis, and poplar (*Populus tremuloides*; Hansen et al., 2007). Clade III is the putative *S*-oxygenation clade and contains what appears to be crucifer-specific radiation of FMOs, which includes the biochemically characterized $FMO_{GS\text{-}OX1}$ (Hansen et al., 2007). In the intervening time, several additional plant genomic sequences became available and allowed for retesting of this *FMO* clade's specificity to crucifers. To do this, we obtained all of the *FMO*s from the genomic sequences of poplar, rice, *Medicago truncatula*, grape (*Vitis vinifera*), and *Physcomitrella patens* and created a complete phylogeny to identify those *FMO*s present in clade III, which has a single ancestor present in *P. patens*. To further extend this analysis, we utilized the $FMO_{GS\text{-}OX}$ and related Arabidopsis sequences to identify all ESTs that were at least 80% identical at the amino acid level. These ESTs identified one potato (*Solanum tuberosum*) FMO, two *Citrus clementine* FMOs, and a set of crucifer FMOs from *Raphanus*, *Brassica*, and *Thalaginella* ssp. (Fig. 2; Supplemental Table S1). Phylogenetic analysis showed that only genomic and EST sequences from the Cruciferae clustered within the $FMO_{GS\text{-}OX}$ subclade, leading us to hypothesize that this is a crucifer-specific clade of FMOs (Fig. 2). Because GSLs are also unique to these plants, these crucifer-specific *FMO*s provide candidate genes for the residual MT to MS *S*-oxygenating enzyme activity present in the $FMO_{GS\text{-}OX1}$ knockout (Hansen et al., 2007). Interestingly, this clade is marked by numerous species-specific duplications as shown by the grape and rice radiations (Fig. 2).

Fine-Scale Mapping of *GS-OX*

Previous quantitative genetics analysis mapped a *GS-OX* locus on Arabidopsis chromosome I in crude proximity to the characterized $FMO_{GS\text{-}OX1}$ (Kliebenstein et al., 2001b; Hansen et al., 2007). This *GS-OX* locus

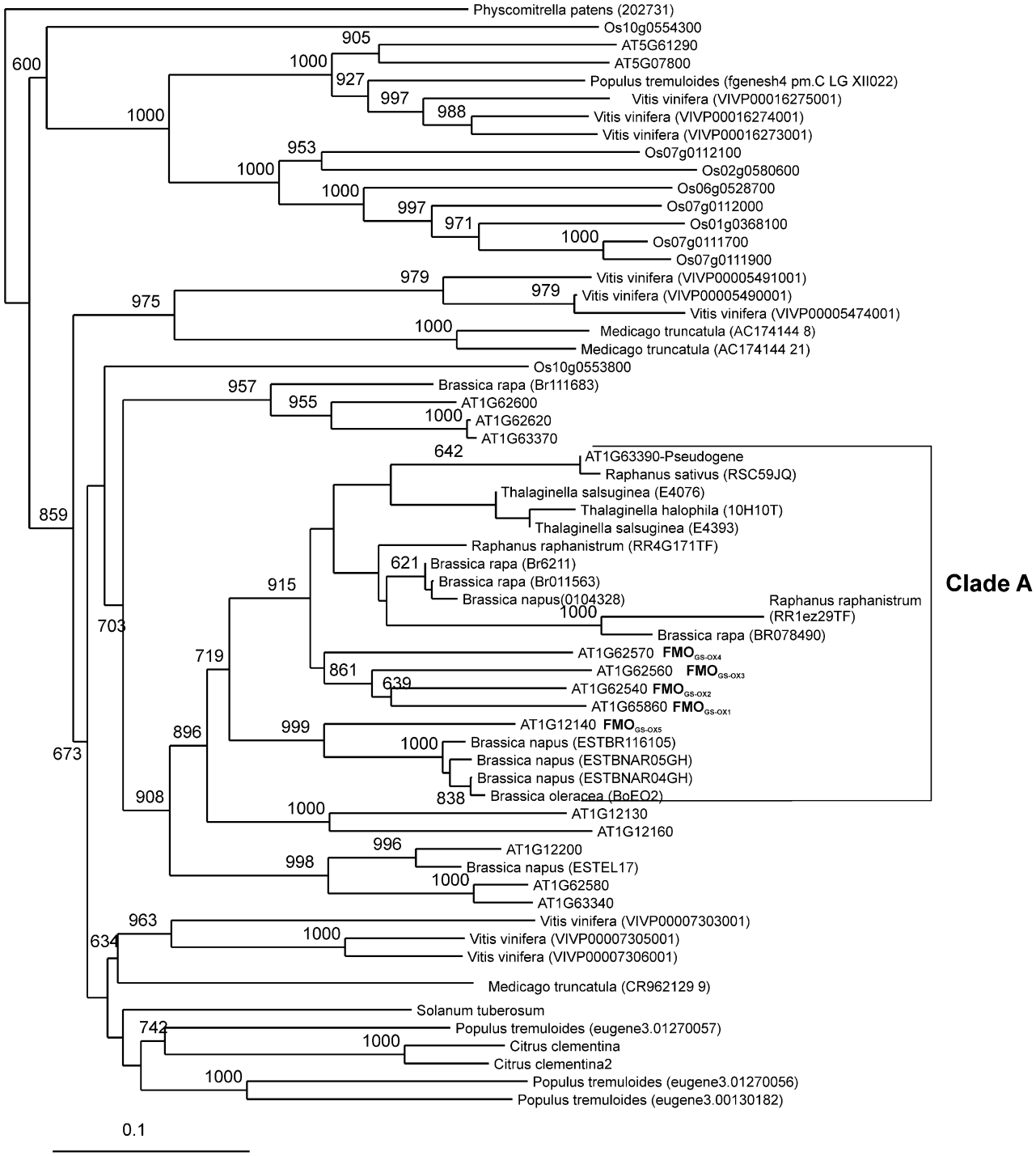

Figure 2. Phylogenetic analysis of $FMO_{GS\text{-}OX}$ homologous sequences. *At1g12140*, *At1g62580*, and *At1g65860* were used to search the available Genomic and EST databases for homologous FMO sequences in clade III (Hansen et al., 2007). The genomic sequences were utilized as full-length proteins. The EST sequences were aligned to identify the minimum unigene set. Clade A, Subclade that appears to be crucifer specific.

controlled differences in the ratio of MT to MS GSLs in the Landsberg *erecta* (L*er*) × Columbia-0 (Col-0) recombinant inbred line (RIL) population (Kliebenstein et al., 2001a). We have conducted a detailed analysis of the existing data in the larger L*er* × Cape Verde Islands (Cvi) and Bay-0 × Shahdara (Sha) RIL populations. This showed that the *GS-OX* locus was in fact two closely linked loci that epistatically control the ratio of MT to MS GSLs (Supplemental Tables S2 and S3; Kliebenstein et al., 2001a; Wentzell et al., 2007). One of

these two loci, as shown by the *GH157* and *F5I14* markers in the L*er* × Cvi and Bay-0 × Sha populations, respectively, was tightly linked to $FMO_{GS\text{-}OX1}$ (*At1g65860*; Fig. 3). Further, the *At1g65860* transcript had a significant cis-expression QTL in the Bay-0 × Sha population that agreed with $FMO_{GS\text{-}OX1}$ likely being the functional basis of one of the two *GS-OX* loci in this region (Wentzell et al., 2007; West et al., 2007). However, this $FMO_{GS\text{-}OX1}$ QTL was not at the genetic position of the originally identified *GS-OX* locus (Kliebenstein et al., 2001b; Fig. 3).

To better resolve the molecular genetic basis of the originally identified *GS-OX* locus, we generated a F_2 population by crossing the L*er* and Wei-0 accessions,

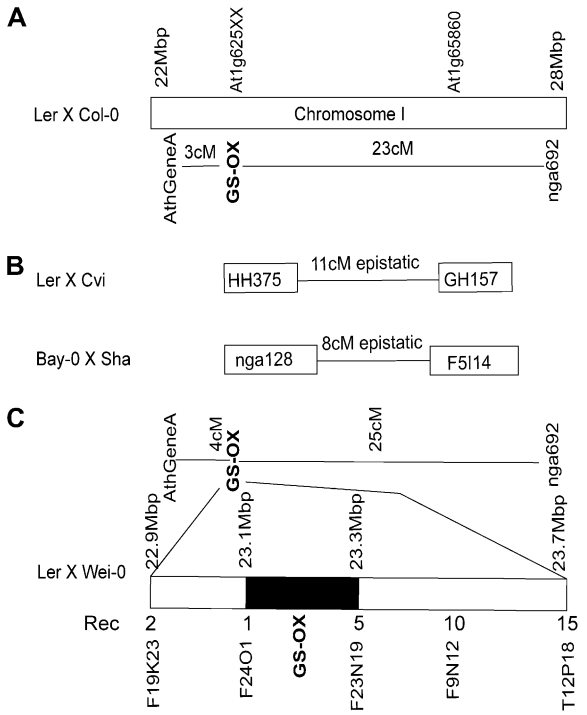

Figure 3. Genetic mapping of GS-OX in multiple Arabidopsis RIL populations. The position of the GS-OX loci [controlling MT:(MT + MS) ratio] on chromosome I in four different Arabidopsis RIL populations is presented. The genomic position of *At1g65860* ($FMO_{GS\text{-}OX1}$) and *At1g62540* to *At1g62580* (*At1g625XX*) is presented for reference. A, For the L*er* × Col-0 population, *GS-OX* was mapped as a qualitative locus and the position is presented in relation to the *AthGeneA* and *nga692* markers. B, In L*er* × Cvi and Bay-0 × Sha, *GS-OX* was mapped as a quantitative trait and the one LOD intervals for the identified loci on chromosome I presented with the genetic distance between them. The tested marker for each QTL is positioned relative to its physical position on chromosome I. Epistatic shows that there was a significant interaction between these two QTLs. C, For the L*er* × Wei-0 F2 population, *GS-OX* was mapped as a qualitative locus and the position is presented in relation to the *AthGeneA* and *nga692* markers. The L*er* × Wei-0 population was used to fine map the major *GS-OX* locus and the fine-mapping information is presented at the bottom with the genomic position of the markers indicated. Rec, Number of recombinations between the given marker and the *GS-OX* phenotype in 400 F_2 individuals. No markers were identified that could further resolve the position of the *GS-OX* locus as indicated by the black box.

which have a strong difference in the *GS-OX* phenotype, but have the same allelic status at the epistatic *GS-Elong* and *GS-AOP* QTLs (Kliebenstein et al., 2001b; Wentzell et al., 2007). This population thereby allowed us to focus on *GS-OX* variation. We genotyped and HPLC phenotyped 400 F_2 individuals and fine-scale mapped the *GS-OX* QTL in this population to a 200-kb region between 23.1 and 23.3 Mb on Arabidopsis chromosome I. This is in the same position as the original *GS-OX* locus from the L*er* × Col-0 population, as well as proximal to the *nga128* and *HH375* markers from the L*er* × Cvi and Bay-0 × Sha populations (Fig. 3; Loudet et al., 2002). This fine-scale map position did not include the $FMO_{GS\text{-}OX1}$ gene, but did include three tandem duplicates that are the closest homologs of $FMO_{GS\text{-}OX1}$, *At1g62540*, *At1g62560*, and *At1g62570* (Fig. 2). Additionally, all three genes had cis-expression QTLs in the available Bay × Sha QTL data, suggesting that gene expression rather than enzyme activity variation in this tandem gene family underlies the *GS-OX* QTL linked to the *nga128* and *HH375* markers in multiple Arabidopsis populations (West et al., 2007). No recombination events between these genes could be identified. The phylogenetic relationship of these *FMO*s to a gene encoding an enzyme that converts MT to MS GSLs, their physical proximity to a locus controlling the conversion of MT to MS GSLs, as well as the presence of expression diversity, led us to hypothesize that these genes are $FMO_{GS\text{-}OX}$s within Arabidopsis. We then proceeded to directly test this biochemical hypothesis on these *FMO*s and on *At1g12140*, which belongs to the proposed $FMO_{GS\text{-}OX}$ clade (Fig. 2).

Recombinant $FMO_{GS\text{-}OX}$s Catalyze the Conversion of MT to MS GSLs

We previously showed that $FMO_{GS\text{-}OX1}$ *S*-oxygenates desulfo and intact MT GSLs, but not other precursors in the Met-derived GSL biosynthesis pathway in Arabidopsis (Hansen et al., 2007). Therefore, we utilized desulfo MT GSLs as substrate to test whether the other Arabidopsis proteins in the $FMO_{GS\text{-}OX}$ subclade catalyzed the *S*-oxygenation of MT to MS GSLs. $FMO_{GS\text{-}OX1}$, $FMO_{GS\text{-}OX2}$, $FMO_{GS\text{-}OX3}$, $FMO_{GS\text{-}OX4}$, and $FMO_{GS\text{-}OX5}$ were individually expressed in *Escherichia coli*. Spheroplasts of *E. coli* expressing these $FMO_{GS\text{-}OX}$ proteins were incubated with desulfo 4-methylthiobutyl (4-MTB) GSL for 1 h, and desulfo GSLs were analyzed by HPLC. Recombinant protein of $FMO_{GS\text{-}OX2}$, $FMO_{GS\text{-}OX3}$, and $FMO_{GS\text{-}OX4}$ all catalyzed the production of desulfo 4-MSB GSL (Fig. 4, C–E) in levels comparable to the $FMO_{GS\text{-}OX1}$ (Fig. 4B). Control spheroplasts transformed with empty vector did not show a significant production of desulfo 4-MSB (Fig. 4A). Recombinant protein of the most distant member of this subclade, $FMO_{GS\text{-}OX5}$, did not convert 4-MTB into 4-MSB (Figs. 2 and 4F). This indicated that either $FMO_{GS\text{-}OX5}$ cannot catalyze the *S*-oxygenation of MT GSLs or it may have substrate specificity for other MT GSLs than 4-MTB.

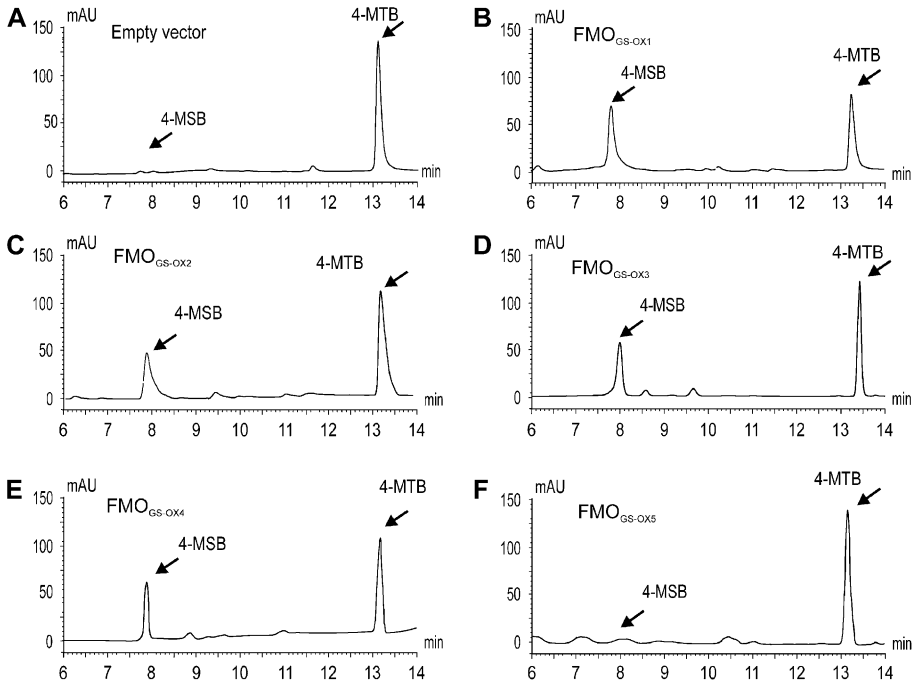

Figure 4. Analysis of *S*-oxygenation activity of $FMO_{GS\text{-}OX1}$ to $FMO_{GS\text{-}OX5}$ for 4-MTB GSL. Spheroplasts of *E. coli* expressing empty vector were used as negative control. A, Negative control; B, assay of $FMO_{GS\text{-}OX1}$; C, assay of $FMO_{GS\text{-}OX2}$; D, assay of $FMO_{GS\text{-}OX3}$; E, assay of $FMO_{GS\text{-}OX4}$; F, assay of $FMO_{GS\text{-}OX5}$. Ratio of 4-MTB:(4-MTB + 4-MSB) was calculated to represent the *S*-oxygenating activity. Significance of the difference between the ratio of 4-MTB:(4-MTB + 4-MSB) for $FMO_{GS\text{-}OX}$ versus the negative control was determined by ANOVA. For $FMO_{GS\text{-}OX1}$ to $FMO_{GS\text{-}OX4}$, $P < 0.001$; for $FMO_{GS\text{-}OX5}$, $P = 0.16$.

The aliphatic, Met-derived GSLs are divided into classes of different side chain lengths: short chain, propyl (C3) and butyl (C4); middle chain, pentyl (C5) and hexyl (C6); and long chain, heptyl (C7) and octyl (C8). Because 4-MTB is the only commercially available MT GSL, we extracted desulfo GSLs from seeds of the Arabidopsis accession Col-0 to use as substrates in the $FMO_{GS\text{-}OX}$ enzyme assay. 4-MTB and 8-MTO GSLs are the dominant GSLs in these seeds. This allowed us to test whether any of the $FMO_{GS\text{-}OX}$s catalyzes the *S*-oxygenation of MT GSLs with chain lengths other than 4-MTB. Spheroplasts of *E. coli* expressing $FMO_{GS\text{-}OX1}$, $FMO_{GS\text{-}OX2}$, $FMO_{GS\text{-}OX3}$, $FMO_{GS\text{-}OX4}$, and $FMO_{GS\text{-}OX5}$ were incubated with the desulfo GSLs derived from seeds, followed by HPLC analyses. Consistent with the previous work, $FMO_{GS\text{-}OX1}$, $FMO_{GS\text{-}OX2}$, $FMO_{GS\text{-}OX3}$, and $FMO_{GS\text{-}OX4}$, but not $FMO_{GS\text{-}OX5}$, catalyzed the conversion of 4-MTB to 4-MSB (Fig. 5, B–F). Interestingly, all five recombinant proteins converted 8-MTO to 8-MSO (Fig. 5, B–F). Thus, $FMO_{GS\text{-}OX1}$, $FMO_{GS\text{-}OX2}$, $FMO_{GS\text{-}OX3}$, and $FMO_{GS\text{-}OX4}$ catalyze the *S*-oxygenating reaction for both short-chain and long-chain MT GSL, whereas $FMO_{GS\text{-}OX5}$ has a more limited substrate specificity as indicated by its specificity for 8-MTO. This suggests that this cluster of FMOs is involved in GSL biosynthesis and that the enzymes have evolved different substrate specificities.

GSL Analyses of $FMO_{GS\text{-}OX}$ Knockout Mutants

To validate the *S*-oxygenation activities of these FMOs in planta, we obtained two independent T-DNA knockout mutants for, respectively, $FMO_{GS\text{-}OX2}$ and $FMO_{GS\text{-}OX4}$, and one T-DNA knockout mutant for, respectively, $FMO_{GS\text{-}OX3}$ and $FMO_{GS\text{-}OX5}$. These T-DNA mutants were confirmed as having no detectable transcript for the corresponding $FMO_{GS\text{-}OX}$ by reverse transcription (RT)-PCR (Supplemental Fig. S1). For each $FMO_{GS\text{-}OX}$ knockout mutant, we measured GSL content in leaves and seeds of segregating progeny obtained from a heterozygous parent (Supplemental Table S4). By analyzing the GSL content in wild-type and homozygous knockout plants in a segregating population derived from a single heterozygous parent, we minimize the influence of potential maternal effects. From the HPLC data, the ratio of MT GSL to the sum of MT and MS GSL, which represents the *S*-oxygenation activity for the conversion from MT GSL to MS GSL, was calculated for each chain length. For $FMO_{GS\text{-}OX2}$ and $FMO_{GS\text{-}OX4}$, there was no statistically significant difference between the MT:(MT + MS) ratios of the two independent T-DNA knockout mutants of the same gene, and the data from the mutants were pooled.

In agreement with predicted biochemistry for $FMO_{GS\text{-}OX2}$, its homozygous knockout mutants showed an increased ratio of MT:(MT + MS) for the butyl, pentyl, heptyl, and octyl Met-derived GSLs in both leaves and seeds in comparison with wild-type plants (Table I). A homozygous knockout mutant in the proposed long-chain-specific $FMO_{GS\text{-}OX5}$ had an increased MT:(MT + MS) for C8 GSLs in seeds, but also for other chain lengths (Table II). This agrees with the observation that only 8-MTO was found to be a substrate for recombinant $FMO_{GS\text{-}OX5}$. The observed changes in the knockout mutants are likely not absolute due to compensatory function present in the other

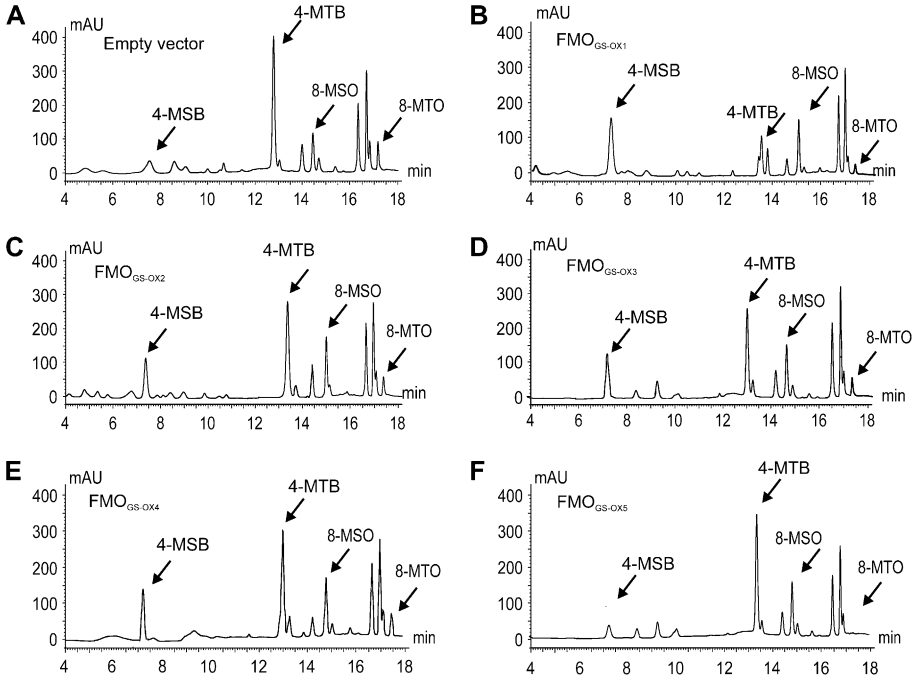

Figure 5. Analysis of *S*-oxygenation activity of $FMO_{GS\text{-}OX1}$ to $FMO_{GS\text{-}OX5}$ for methythioalkyl GSL. The activity of each recombinant $FMO_{GS\text{-}OX}$ was detected in assays using desulfo GSL extracts from Arabidopsis seed with a final concentration of 2 mM total desulfo GSL as substrate. Spheroplasts of *E. coli* expressing empty vector were used as negative control. A, Negative control; B, assay of $FMO_{GS\text{-}OX1}$; C, assay of $FMO_{GS\text{-}OX2}$; D, assay of $FMO_{GS\text{-}OX3}$; E, assay of $FMO_{GS\text{-}OX4}$; F, assay of $FMO_{GS\text{-}OX5}$. Ratio of 4-MTB:(4-MTB + 4-MSB) was calculated to represent the *S*-oxygenating activity for short-chain GSL. The significance of the difference between the ratio 4-MTB:(4-MTB + 4-MSB) of the respective $FMO_{GS\text{-}OX}$ and the negative control was determined by ANOVA. For $FMO_{GS\text{-}OX1}$ to $FMO_{GS\text{-}OX4}$, $P < 0.001$; for $FMO_{GS\text{-}OX5}$, $P = 0.304$. Ratio of 8-MTO:(8-MTO + 8-MSO) was calculated to represent the *S*-oxygenating activity for long-chain GSL. The significance of the difference between the ratio 8-MTO:(8-MTO + 8-MSO) of the respective $FMO_{GS\text{-}OX}$ and the negative control was determined by ANOVA. For $FMO_{GS\text{-}OX1}$ to $FMO_{GS\text{-}OX5}$, $P < 0.001$.

functioning $FMO_{GS\text{-}OX}$s. In contrast, the T-DNA knockout mutant of *$FMO_{GS\text{-}OX4}$* did not show an increase in MT:(MT + MS) in either leaves or seeds (Table III). This may be due to low expression or low in planta activity in the Col-0 accession, in which case a mutant phenotype will be hidden by functional redundancy with the other $FMO_{GS\text{-}OX}$s.

The only available T-DNA knockout mutant for *$FMO_{GS\text{-}OX3}$* is in the L*er* accession. In contrast to the Col-0 accession, L*er* has predominantly propyl C3 instead of butyl C4 Met-derived GSLs (Kliebenstein et al., 2001b). Another difference between the two ecotypes is that L*er* expresses a functional AOP3 (2-oxoglutarate-dependent dioxygenase; Kliebenstein

Table I. *Altered GS-OX activity in the $FMO_{GS\text{-}OX2}$ T-DNA mutant*

GSL content in seeds and leaves was analyzed. All plants were segregants derived from a parental line heterozygous for the T-DNA knockout allele. MT:(MS + MT) represents the *S*-oxygenation activity for the conversion from MT GSL to MS GSL. This T-DNA mutant is in a wild-type Col-0 background.

MT:(MS + MT)	Leaf Tissue					Seed Tissue				
	Homozygous Knockout (n^a = 52)		Homozygous Wild Type (n = 36)		P^d	Homozygous Knockout (n = 24)		Homozygous Wild Type (n = 24)		P
	Mean[b]	SE[c]	Mean	SE		Mean	SE	Mean	SE	
Propyl GSL (C3)	0.12	0.008	0.13	0.011	NS[e]	ND		ND[f]		
Butyl GSL (C4)	0.33	0.011	0.24	0.013	<0.001	0.70	0.008	0.60	0.023	0.001
Pentyl GSL (C5)	0.24	0.013	0.17	0.015	<0.001	0.79	0.024	0.73	0.040	<0.001
Hexyl GSL (C6)	ND		ND			ND		ND		
Heptyl GSL (C7)	0.24	0.009	0.22	0.016	<0.001	0.54	0.034	0.51	0.030	0.001
Octyl GSL (C8)	0.10	0.005	0.09	0.008	0.001	0.32	0.014	0.29	0.022	0.003

[a]Number of individual lines measured per genotype class. [b]Mean is the mean value of MT:(MS + MT). [c]Standard error for the mean value. [d]*P* value for GSL differences between the two genotypes as determined by ANOVA. [e]Nonsignificant *P* values ($P > 0.05$). [f]Given GSL was not detectable; therefore, no statistical analyses were conducted.

Table II. *Altered GS-OX activity in the $FMO_{GS\text{-}OX5}$ T-DNA mutant*

GSL content in seeds and leaves was analyzed. All plants were segregants derived from a parental line heterozygous for the T-DNA knockout allele. MT:(MS + MT) represents the *S*-oxygenation activity for the conversion from MT GSL to MS GSL. This T-DNA mutant is in a wild-type Col-0 background.

MT:(MS + MT)	Leaf Tissue					Seed Tissue				
	Homozygous Knockout (n^a = 35)		Homozygous Wild Type (n = 29)		P^d	Homozygous Knockout (n = 29)		Homozygous Wild Type (n = 26)		P
	Mean[b]	SE[c]	Mean	SE		Mean	SE	Mean	SE	
Propyl GSL (C3)	ND[e]		ND			0.03	0.000	0.03	0.000	NS
Butyl GSL (C4)	0.20	0.000	0.20	0.000	NS[f]	0.80	0.010	0.79	0.010	NS
Pentyl GSL (C5)	ND		ND			0.91	0.010	0.90	0.010	NS
Hexyl GSL (C6)	ND		ND			ND		ND		
Heptyl GSL (C7)	0.20	0.020	0.20	0.030	NS	ND		ND		
Octyl GSL (C8)	0.27	0.040	0.28	0.050	NS	0.39	0.010	0.37	0.010	<0.001

[a]Number of individual lines measured per genotype class. [b]Mean value of MT:(MS + MT). [c]Standard error for the mean value. [d]*P* value for GSL differences between the two genotypes as determined by ANOVA. [e]Given GSL was not detectable; therefore, no statistical analyses were conducted. [f]Nonsignificant *P* values ($P > 0.05$).

et al., 2001c), which catalyzes the conversion from MS GSL to hydroxyalkyl (OH) GSL (Fig. 1). This results in accumulation of OH GSL instead of MS GSL in L*er*. Therefore, the ratio of MT GSL to the sum of MT and OH GSLs was used as a measure for *GS-OX* activity in L*er*. Significant increase of 3-MT:(3-MT + 3-OH) was observed in both leaves and seeds in homozygous knockout mutants compared to wild-type plants (Table IV). No significant difference was found for other MT GSLs in this knockout mutant, which suggests a preference of $FMO_{GS\text{-}OX3}$ for short-chain MT GSLs in L*er*. In our data, there is agreement between the in vitro and in planta activities for the majority of $FMO_{GS\text{-}OX}$s.

Ratio of MT:(MT + MS) Decreased in $FMO_{GS\text{-}OX}$ Overexpressers

To further complement the in vitro data, we individually overexpressed all four *FMO*s in Col-0. For each $35S::FMO_{GS\text{-}OX}$ construct, two independent T_1 lines were identified, segregants from these lines were genotyped, and GSLs measured from leaves and seeds of homozygotes and wild-type offspring (Supplemental Table S5). The ratio of MT:(MT + MS) was calculated for each chain length to estimate the GS-OX activity. There was no statistically significant difference between the two independent transgenic lines for any $35S::FMO_{GS\text{-}OX}$ construct, and therefore data from the two lines were pooled.

In leaves, MT GSLs were extensively converted into MS GSLs in the $35S::FMO_{GS\text{-}OX2}$ and $35S::FMO_{GS\text{-}OX3}$ lines, resulting in a significant decrease of the MT:(MT + MS) ratio in comparison to the wild type (Tables V and VI). In seeds of the $35S::FMO_{GS\text{-}OX3}$, all MT GSLs were converted to MS GSLs, whereas only the short-chain butyl C4 Met-derived GSL showed a slight decrease in MT:(MT + MS) ratio in the seeds of $35S::FMO_{GS\text{-}OX2}$ (Tables V and VI). These data, combined with the T-DNA and in vitro analysis, suggest that, whereas these two genes are both $FMO_{GS\text{-}OX}$ enzymes, they have slightly different specificities.

$35S::FMO_{GS\text{-}OX4}$ did not show a decrease in the ratio of MT:(MT + MS) either in leaves or in seeds (Table

Table III. *Altered GS-OX activity in the $FMO_{GS\text{-}OX4}$ T-DNA mutant*

GSL content in seeds and leaves was analyzed. All plants were segregants derived from a parental line heterozygous for the T-DNA knockout allele. MT:(MS + MT) represents the *S*-oxygenation activity for the conversion from MT GSL to MS GSL. This T-DNA mutant is in a wild-type Col-0 background.

MT:(MS + MT)	Leaf Tissue					Seed Tissue				
	Homozygous Knockout (n^a = 40)		Homozygous Wild Type (n = 37)		P^d	Homozygous Knockout (n = 23)		Homozygous Wild Type (n = 24)		P
	Mean[b]	SE[c]	Mean	SE		Mean	SE	Mean	SE	
Propyl GSL (C3)	0.26	0.020	0.24	0.020	NS[e]	ND[f]		ND		
Butyl GSL (C4)	0.41	0.020	0.39	0.020	NS	0.72	0.010	0.71	0.010	NS
Pentyl GSL (C5)	0.23	0.020	0.22	0.020	NS	0.79	0.020	0.76	0.020	NS
Hexyl GSL (C6)	ND		ND			ND		ND		
Heptyl GSL (C7)	0.25	0.010	0.23	0.010	NS	0.62	0.020	0.58	0.030	NS
Octyl GSL (C8)	0.11	0.010	0.12	0.010	NS	0.32	0.010	0.31	0.010	NS

[a]Number of individual lines measured per genotype class. [b]Mean value of MT:(MS + MT). [c]Standard error for the mean value. [d]*P* value for GSL differences between the two genotypes as determined by ANOVA. [e]Nonsignificant *P* values ($P > 0.05$). [f]Given GSL was not detectable; therefore, no statistical analyses were conducted.

Table IV. *Altered GS-OX activity in the $FMO_{GS\text{-}OX3}$ T-DNA mutant*

GSL content in seeds and leaves was analyzed. All plants were segregants derived from a parental line heterozygous for the T-DNA knockout allele. MT:(OH + MT) represents the *S*-oxygenation activity for the conversion from MT GSL to MS GSL. This T-DNA mutant is in a wild-type L*er* background.

MT:(OH + MT)	Leaf Tissue					Seed Tissue				
	Homozygous Knockout (n[a] = 21)		Homozygous Wild Type (n = 26)		P[d]	Homozygous Knockout (n = 17)		Homozygous Wild Type (n = 19)		P
	Mean[b]	SE[c]	Mean	SE		Mean	SE	Mean	SE	
Propyl GSL (C3)	0.38	0.020	0.02	0.020	<0.001	0.72	0.030	0.21	0.020	<0.001
Butyl GSL (C4)	ND[e]		ND			ND		ND		
Pentyl GSL (C5)	ND		ND			ND		ND		
Hexyl GSL (C6)	ND		ND			ND		ND		
Heptyl GSL (C7)	ND		ND			0.74	0.040	0.72	0.040	NS
Octyl GSL (C8)	0.11	0.010	0.09	0.010	NS[f]	0.64	0.030	0.56	0.030	NS

[a]Number of individual lines measured per genotype class. [b]Mean value of MT:(MS + MT). [c]Standard error for the mean value. [d]*P* value for GSL differences between the two genotypes as determined by ANOVA. [e]ND, GSL was not detectable; therefore, no statistical analyses were conducted. [f]NS, Nonsignificant *P* values ($P > 0.05$).

VII). For C4 GSLs, a very slight, but statistically significant, increase of MT:(MT + MS) was detected, indicating a possible repression of the conversion from 4-MTB to 4-MSB. As with the other $FMO_{GS\text{-}OX}$ overexpresser data, the *35S::*$FMO_{GS\text{-}OX4}$ data were derived from two independent, segregating T_1 transgenic overexpression lines that exhibited a significant decrease of the MT:(MT + MS) ratio in comparison to wild-type plants (Supplemental Fig. S2; Supplemental Table S6). This suggests that $FMO_{GS\text{-}OX4}$ catalyzes the *S*-oxygenation reaction and that the *35S::*$FMO_{GS\text{-}OX4}$ transgene was silenced in the T_2 generation.

In agreement with its predicted substrate specificity, *35S::*$FMO_{GS\text{-}OX5}$ lines had a significant decrease of MT:(MT + MS) for only octyl C8 GSL in seeds compared to wild type (Table VIII). Interestingly, 7-methylthioheptyl (7-MTH) GSL, another long-chain MT GSL, had a similar concentration as 8-MTO in seeds of the wild-type plant, but we did not detect any 7-MSH GSL, indicating that no significant conversion from 7-MTH to 7-MSH occurred in *35S::*$FMO_{GS\text{-}OX5}$ (Supplemental Table S5). This confirmed that $FMO_{GS\text{-}OX5}$ is specific for the 8-MTO GSL substrate.

DISCUSSION

Modifications of the GSL side chain are of particular importance because the biological activity of the GSL hydrolysis products is determined to a large extent by the structure of the side chain. We identified four new *FMO* genes encoding for enzymes capable of *S*-oxygenating aliphatic GSLs. Three of these *FMO*s, $FMO_{GS\text{-}OX2}$ to $FMO_{GS\text{-}OX4}$, were identified by fine mapping of a 200-kb region containing a *GS-OX* QTL on chromosome I in a L*er* × Wei-0 F_2 population. The three *FMO*s clustered together with $FMO_{GS\text{-}OX5}$ and the previously characterized $FMO_{GS\text{-}OX1}$ in a subclade that appears to be crucifer specific. $FMO_{GS\text{-}OX2}$, $FMO_{GS\text{-}OX3}$, and $FMO_{GS\text{-}OX4}$ *S*-oxygenated all available MT GSLs as did $FMO_{GS\text{-}OX1}$, whereas $FMO_{GS\text{-}OX5}$ showed high substrate specificity to 8-MTO GSL.

Substrate Specificity of $FMO_{GS\text{-}OX}$s

In animals, there are five functionally expressed *FMO* genes that detoxify a vast spectrum of xenobiotics. This vast spectrum is due to broad substrate

Table V. *Altered GS-OX activity in the $FMO_{GS\text{-}OX2}$ overexpression lines*

GSL content in seeds and leaves was analyzed. All plants were segregants derived from two independent T_1 generation *35S::*$FMO_{GS\text{-}OX2}$ lines. MT:(MS + MT) represents the *S*-oxygenation activity for the conversion from MT GSL to MS GSL.

MT:(MS + MT)	Leaf Tissue					Seed Tissue				
	35S::$FMO_{GS\text{-}OX2}$ (n[a] = 46)		Col-0 (n = 24)		P_{gene}[d]	*35S::*$FMO_{GS\text{-}OX2}$ (n = 23)		Col-0 (n = 18)		P_{gene}
	Mean[b]	SE[c]	Mean	SE		Mean	SE	Mean	SE	
Propyl GSL (C3)	0.07	0.002	0.08	0.006	<0.001	ND[e]		ND		
Butyl GSL (C4)	0.18	0.004	0.34	0.013	<0.001	0.67	0.013	0.71	0.011	0.046
Pentyl GSL (C5)	0.03	0.014	0.47	0.015	<0.001	0.73	0.024	0.76	0.017	NS[f]
Hexyl GSL (C6)	ND		ND			ND		ND		
Heptyl GSL (C7)	0.08	0.011	0.37	0.016	<0.001	0.52	0.031	0.54	0.031	NS
Octyl GSL (C8)	0.03	0.006	0.19	0.009	<0.002	0.32	0.015	0.32	0.010	NS

[a]Number of individual lines measured per genotype class. [b]Mean value of MT:(MS + MT). [c]Standard error for the mean value. [d]*P* value for GSL differences between the two genotypes as determined by ANOVA. [e]Given GSL was not detectable; therefore, no statistical analyses were conducted. [f]Nonsignificant *P* values ($P > 0.05$).

Table VI. *Altered GS-OX activity in the $FMO_{GS\text{-}OX3}$ overexpression lines*

GSL content in seeds and leaves was analyzed. All plants were segregants derived from two independent T_1 generation *35S::$FMO_{GS\text{-}OX3}$* lines. MT:(MS + MT) represents the *S*-oxygenation activity for the conversion from MT GSL to MS GSL.

MT:(MS + MT)	Leaf Tissue					Seed Tissue				
	35S::$FMO_{GS\text{-}OX3}$ (n^a = 19)		Col-0 (n = 13)		P^d_{gene}	*35S::$FMO_{GS\text{-}OX3}$* (n = 12)		Col-0 (n = 8)		P_{gene}
	Mean[b]	SE[c]	Mean	SE		Mean	SE	Mean	SE	
Propyl GSL (C3)	0.05	0.000	0.12	0.010	<0.001	0.01	0.000	0.03	0.000	<0.001
Butyl GSL (C4)	0.02	0.000	0.22	0.020	<0.001	0.35	0.020	0.74	0.020	<0.001
Pentyl GSL (C5)	0.03	0.010	0.31	0.030	<0.001	0.48	0.030	0.83	0.020	<0.001
Hexyl GSL (C6)	ND[e]		ND			0.13	0.020	0.33	0.030	<0.001
Heptyl GSL (C7)	0.07	0.020	0.29	0.040	<0.001	0.35	0.020	0.63	0.020	<0.001
Octyl GSL (C8)	0.04	0.010	0.18	0.020	<0.001	0.15	0.010	0.33	0.010	<0.001

[a]Number of individual lines measured per genotype class. [b]Mean value of MT:(MS + MT). [c]Standard error for the mean value. [d]*P* value for GSL differences between the two genotypes as determined by ANOVA. [e]Given GSL was not detectable; therefore, no statistical analyses were conducted.

specificity that makes the mammalian FMOs capable of oxidizing thousands of plant natural products as well as thousands of synthetic therapeutic drugs (Krueger and Williams, 2005; Cashman and Zhang, 2006). Plants, on the other hand, have many more *FMO* genes, possibly with more restricted substrate specificity. In Arabidopsis, there are 29 genes with homology to known *FMO*s (Schlaich, 2007). The enzyme $FMO_{GS\text{-}OX1}$ was shown to have substrate specificity in that it required an *S*-Glc group on its substrates (Hansen et al., 2007). $FMO_{GS\text{-}OX1}$ *S*-oxygenated desulfo and intact GSLs, but not the structurally related Met and aldoxime that do not contain an *S*-Glc group. In this article, we show additional substrate specificity in plant FMOs because we found that $FMO_{GS\text{-}OX5}$ is specific for long-chain aliphatic GSLs. This indicates that the *S*-Glc group is not the only structural requirement for the substrate of $FMO_{GS\text{-}OX5}$. Size restriction might be another factor determining substrate specificity whereby $FMO_{GS\text{-}OX5}$ excludes the short-chain GSLs.

It is reported that when there is no available substrate, the FMO proteins exist as 4α-hydroperoxy flavin, which is a precharged complex containing a reduced form of fatty acid dehydrogenase and NADPH that is ready to act on substrates (Eswaramoorthy et al., 2006). The 4α-hydroperoxy flavin complex of $FMO_{GS\text{-}OX5}$ may have a tertiary structure in the binding site that only fits with 8-MTO and prevents shorter chain-length MT GSLs from either entering or being properly held by the enzyme. However, the mechanism of the conformational and chemical complementarities between the MT GSLs and $FMO_{GS\text{-}OX}$ enzymes remains to be shown.

The phylogenetic tree of plant *FMO*s in rice, poplar, and Arabidopsis contains three clades (Hansen et al., 2007). Our phylogenetic analysis of $FMO_{GS\text{-}OX}$ homologs (Fig. 2) is based on the genomic sequences present in clade III and EST sequences with more than 80% identity to at least one of the three FMOs used for database searching. In this proposed *S*-oxygenation clade III (Fig. 2), *$FMO_{GS\text{-}OX1}$* to *$FMO_{GS\text{-}OX5}$* are the only characterized genes. Given that poplar, rice, alfalfa (*Medicago sativa*), grape, tomato (*Solanum lycopersicum*), lemon (*Citrus limon*), and moss do not produce GSLs, other *FMO*s in this clade may be involved in *S*-oxygenation for a diversity of sulfur-containing

Table VII. *Altered GS-OX activity in the $FMO_{GS\text{-}OX4}$ overexpression lines*

GSL content in seeds and leaves was analyzed. All plants were segregants derived from two independent T_1 generation *35S::$FMO_{GS\text{-}OX4}$* lines. MT:(MS + MT) represents the *S*-oxygenation activity for the conversion from MT GSL to MS GSL.

MT:(MS + MT)	Leaf Tissue					Seed Tissue				
	35S::$FMO_{GS\text{-}OX4}$ (n^a = 66)		Col-0 (n = 23)		P^d_{gene}	*35S::$FMO_{GS\text{-}OX4}$* (n = 13)		Col-0 (n = 6)		P_{gene}
	Mean[b]	SE[c]	Mean	SE		Mean	SE	Mean	SE	
Propyl GSL (C3)	0.13	0.010	0.13	0.010	NS[e]	ND		ND		
Butyl GSL (C4)	0.26	0.010	0.25	0.010	0.001	0.75	0.040	0.74	0.050	0.030
Pentyl GSL (C5)	0.22	0.010	0.22	0.010	NS	ND		ND		
Hexyl GSL (C6)	ND[f]		ND			ND		ND		
Heptyl GSL (C7)	0.26	0.010	0.25	0.010	NS	0.37	0.040	0.30	0.080	NS
Octyl GSL (C8)	0.14	0.010	0.14	0.010	NS	0.21	0.030	0.18	0.050	NS

[a]Number of individual lines measured per genotype class. [b]Mean value of MT:(MS + MT). [c]Standard error for the mean value. [d]*P* value for GSL differences between the two genotypes as determined by ANOVA. [e]Nonsignificant *P* values ($P > 0.05$). [f]Given GSL was not detectable; therefore, no statistical analyses were conducted.

Table VIII. *Altered GS-OX activity in the $FMO_{GS\text{-}OX5}$ overexpression lines*

GSL content in seeds and leaves was analyzed. All plants were segregants derived from two independent T_1 generation *35S::FMO*$_{GS\text{-}OX5}$ lines. MT:(MS + MT) represents the *S*-oxygenation activity for the conversion from MT GSL to MS GSL.

MT:(MS + MT)	Leaf Tissue					Seed Tissue				
	35S::FMO$_{GS\text{-}OX5}$ (n[a] = 40)		Col-0 (n = 36)		P^{d}_{gene}	*35S::FMO*$_{GS\text{-}OX5}$ (n = 28)		Col-0 (n = 30)		P_{gene}
	Mean[b]	SE[c]	Mean	SE		Mean	SE	Mean	SE	
Propyl GSL (C3)	ND[e]		ND			0.03	0.000	0.03	0.000	NS
Butyl GSL (C4)	0.22	0.000	0.30	0.000	0.017	0.82	0.010	0.72	0.040	NS
Pentyl GSL (C5)	ND		ND			0.90	0.010	0.94	0.010	NS
Hexyl GSL (C6)	ND		ND			ND		ND		
Heptyl GSL (C7)	0.13	0.030	0.14	0.020	NS[f]	ND		ND		
Octyl GSL (C8)	0.11	0.000	0.11	0.000	NS	0.14	0.020	0.34	0.020	<0.001

[a]Number of individual lines measured per genotype class. [b]Mean value of MT:(MS + MT). [c]Standard error for the mean value. [d]*P* value for GSL differences between the two genotypes as determined by ANOVA. [e]Given GSL was not detectable; therefore, no statistical analyses were conducted. [f]Nonsignificant *P* values ($P > 0.05$).

compounds and therefore contribute to a diversity of biological functions (Fig. 2).

Possible Biological Function of $FMO_{GS\text{-}OX}$s

We have shown that the biochemical function of the $FMO_{GS\text{-}OX}$s is to catalyze the *S*-oxygenation of the endogenous substrate MT GSL to MS GSL. The physiological function of $FMO_{GS\text{-}OX}$s depends on the biological activity of the hydrolysis products of the MS GSLs and of further modified GSLs. For humans, the isothiocyanate hydrolysis products of 4-MSB, 7-MSH, and 8-MSO GSLs have been shown to be strong inducers of phase II enzymes and thereby function as cancer-preventing agents (Rose et al., 2000; Fahey et al., 2002). In planta, MS GSLs have been shown to play a role in protection against insects (Rohr et al., 2006), and the isothiocyanate derived from 4-MSB GSL has been shown to play a role in protecting Arabidopsis against pathogens (Tierens et al., 2001). This indicates that $FMO_{GS\text{-}OX}$s are important for plant defense responses. In some Arabidopsis accessions, MS GSLs can be converted to OH, alkenyl, hydroxylalkenyl, and benzoyloxy GSLs (Fig. 1), adding more layers of complexity to the warfare between Arabidopsis and its enemies (Kliebenstein et al., 2001c; Tierens et al., 2001). The plants overexpressing $FMO_{GS\text{-}OX}$s showed significant increases in the accumulation of MS GSLs at the expense of the MT GSLs. This indicates that the production of MS GSLs and the further modified GSLs downstream in the pathway (Fig. 1) require the $FMO_{GS\text{-}OX}$ proteins. This is an important consideration when $FMO_{GS\text{-}OX}$s are utilized in breeding and genetic engineering toward plants with a high level of cancer-preventive methylsulfinylalkyl isothiocyanates, increased pathogen resistance, or decreased level of the deleterious downstream GSLs, such as progoitrin, 2-hydroxy-but-3-enyl GSL (Kliebenstein et al., 2001a; Halkier and Gershenzon 2006). In addition, when altering plants via breeding or engineering approaches toward isothiocyanates of MS GSLs, it is important to also incorporate genes affecting the breakdown of GSLs into the scheme to ensure that isothiocyanates are produced.

Gene Duplication and Evolution of $FMO_{GS\text{-}OX}$s

The Arabidopsis $FMO_{GS\text{-}OX}$s are present in three gene clusters that appear to have evolved through a combination of local tandem duplication, whole-genome duplications, and a distal duplication (Fig. 2; Vision et al., 2000; Blanc and Wolfe 2004; Rizzon et al., 2006). Interestingly, this group of FMOs may represent crucifer-specific radiation because we have to date only identified cruciferous genes to reside within this $FMO_{GS\text{-}OX}$ subclade. Whereas we utilized all available sequence databases, further work is required to fully validate whether this is in fact crucifer-specific radiation associated with the evolution of GSL biosynthesis. Thus, this *FMO* subclade begins to allow potential detailed analysis of how gene duplicates can either partition the original function (subfunctionalization) or derive entirely new functions (neofunctionalization; Lynch and Conery, 2000). In the Arabidopsis $FMO_{GS\text{-}OX}$ part of this *FMO* subclade, there is evidence for subfunctionalization; however, the true direction of this process will require the identification and biochemical characterization of $FMO_{GS\text{-}OX}$ ancestral genes in species basal to the Cruciferae. Phylogenetic analysis suggests that there might be a precursor $FMO_{GS\text{-}OX}$, which first duplicated into $FMO_{GS\text{-}OX5}$ and a $FMO_{GS\text{-}OX1}$ to $FMO_{GS\text{-}OX4}$ precursor. The different substrate specificity between $FMO_{GS\text{-}OX5}$ and $FMO_{GS\text{-}OX1}$ to $FMO_{GS\text{-}OX4}$ is potentially an instance of biochemical subfunctionalization whereby $FMO_{GS\text{-}OX5}$ is likely subfunctionalized for long chain-length substrate, whereas $FMO_{GS\text{-}OX1}$ to $FMO_{GS\text{-}OX4}$ retained broad chain-length specificity from the precursor protein. Further subfunctionalization, potentially from tissue-specific expression patterns, can also be found within $FMO_{GS\text{-}OX1}$ to $FMO_{GS\text{-}OX4}$ and is evidenced by the knockout mutant analysis where both $FMO_{GS\text{-}OX1}$ and $FMO_{GS\text{-}OX2}$ control 8-MSO pro-

duction in planta, whereas $FMO_{GS\text{-}OX3}$, which is capable of catalyzing this reaction in vitro, does not control this reaction in planta (Tables I and II; Hansen et al., 2007). These slight differences between $FMO_{GS\text{-}OX}$ genes might be explained by analysis of microarray data (http://www.genevestigator.ethz.ch; Zimmermann et al., 2004) showing that these genes have different expression patterns across organs and growth stages. Specific identification and validation of the tissue expression patterns of these $FMO_{GS\text{-}OX}$s and the substrates for the other members of this FMO clade could help our understanding of how and when duplicates undergo either biochemical or expression-based subfunctionalization.

Gene Duplication and Quantitative Genetic Variation

The association of the duplicated $FMO_{GS\text{-}OX}$s with independent QTLs for the *S*-oxygenation reaction in Arabidopsis raises another possible role for duplicated gene families (Fig. 2). Duplicated gene families, while providing redundancy to a system, may also enhance the potential for quantitative variation within a trait. This is illustrated by the fact that each of the $FMO_{GS\text{-}OX}$s has a large expression polymorphism, yet there is only quantitative variation for this trait rather than qualitative. As such, the large polymorphisms in each independent gene are dampened by the presence of the other genes. While duplicated genes do show enhanced levels of genetic variation as would be expected under this model (Gu et al., 2004; Kliebenstein, 2008), it remains to be seen whether duplicated gene families show any bias in controlling quantitative trait variation.

In summary, identification of *S*-oxygenating activity of the $FMO_{GS\text{-}OX}$s may impact both applied and basic research fields. These genes can potentially be applied in genetic engineering for the production of 4-MSB, 7-MSH, and 8-MSO GSLs, or removal of 2-hydroxybut-3-enyl GSL. In addition, the characterization of the $FMO_{GS\text{-}OX}$s will help to gain more biochemical insight into plant FMO proteins, which we have just begun to learn about, and it may also bring clues for the functions of the noncharacterized plant FMOs. Finally, this well-defined gene family may provide an optimal model for studying neo- versus subfunctionalization following gene duplication.

MATERIALS AND METHODS

Generation of Phylogenetic Tree

The entire FMO complement from the genomic sequence for *Medicago truncatula*, grape (*Vitis vinifera*), *Physcomitrella patens*, rice (*Oryza sativa*), Arabidopsis (*Arabidopsis thaliana*), and poplar (*Populus tremuloides*) were obtained and translated into their corresponding amino acid sequence. Gene abbreviations are per genome consortium convention or previous publication (Hansen et al., 2007; Supplemental Fig. S1). All FMO amino acid sequences were used to construct a complete neighbor-joining tree with 1,000 bootstraps in ClustalX. The *P. patens* sequence most closely associated with $FMO_{GS\text{-}OX1}$ was used to define the *S*-oxygenation subclade for further analysis (Fig. 2). This subclade includes all previous poplar and rice sequences predicted to be within the *S*-oxygenation subclade. We then identified all EST sequences showing at least 80% amino acid identity with one of three *FMO*s and included these in the phylogenetic analysis. All of these EST sequences clustered within the *P. patens* sequence on an unrooted cladogram containing all sequences and, as such, we utilized the *P. patens* sequence as a root for the presented cladogram focused on the *S*-oxygenation subclade (Fig. 2). Only those branches with at least 600 of 1,000 bootstrap support are labeled.

Genetic Mapping of GS-OX

The accessions L*er* and Wei-0 of Arabidopsis were crossed and the resulting F_1 selfed to generate an F_2 mapping population. These accessions were chosen because they have the same alleles at the *AOP* and *Elong* loci and thereby the only aliphatic GSL structural polymorphism between these accessions is a *GS-OX* polymorphism (Kliebenstein et al., 2001b; Burow et al., 2008). Four hundred F_2 plants were screened for recombination events between the *AthGeneA* and *nga692* markers on chromosome I using a previously described high-throughput DNA extraction and PCR protocol (Kliebenstein et al., 2001b, 2001c). GSLs were analyzed via HPLC for all 400 lines. All recombinant F_2 were selfed and eight F_3 progeny tested from each parent to assess segregation of the *GS-OX* phenotype to confirm the parental genotype at *GS-OX*. Microsatellite markers were made using available genomic sequence for fine-scale mapping. These markers were F19K23 (F, GGTCTAATTGCCGTTGTTGC; R, GAATTCTGTAACATCCCATTTCC), F23N19 (F, TTCCACACTTTCACCGATCA; R, GCTTTTGTTTCTCCCCTTCC), F9N12 (F, CGAGTCTAGAAACTCCGGTGA; R, TCAGCGTAAACCGTCTTTCC); T12P18 (F, GAGAGTCTTCTATTAGAAG; R, CAAATTTGTTAATGTGCGTG); and F24O1 (F, TGCTTCAAGCCCAAGCTTAT; R, AGCGGCAAGAGGAAGTATGA). All recombinant F_2 progeny were genotyped with these markers to resolve the position of *GS-OX*.

Previous HPLC data on GSL accumulation in the leaves and seeds of the L*er* × Cvi RILs was reanalyzed to measure the GS-OX phenotype for the short-chain aliphatic GSLs (Supplemental Tables S2 and S3; Kliebenstein et al., 2001a). QTL cartographer was used to map QTLs for this trait as previously described and ANOVA utilized to test the significant QTLs for an impact on the short-chain GS-OX phenotype (Kliebenstein et al., 2001a). The same ANOVA was used to test for epistatic interactions between significant QTLs using the previously published Bay-0 × Sha GSL data (Wentzell et al., 2007).

Heterologous Expression of $FMO_{GS\text{-}OX}$ Proteins in *Escherichia coli*

The coding sequences of the four $FMO_{GS\text{-}OX}$s were amplified by RT-PCR. Total plant RNA was isolated with TRIzol (Invitrogen) according to the manufacturer's recommendations. First-strand cDNA was synthesized using the iScript cDNA synthesis kit (Bio-Rad). The coding sequence of $FMO_{GS\text{-}OX2}$ (*At1g62540*) was amplified from first-strand cDNA with the following primers: 5′-ATGGCACCAGCTCAAAACCC-3′ and 5′-GAGGATATGGGAAGGATG GAAACTAAT-3′. The coding sequence of $FMO_{GS\text{-}OX3}$ (*At1g62560*) was amplified with the following primers: 5′-ATGGCACCAGCTCAAAACCAAATC-3′ and 5′-TCTTCCATTTTCGAGGTAATAAG-3′. The coding sequence of $FMO_{GS\text{-}OX4}$ (*At1g62570*) was amplified with the following primers: 5′-ATGGCACCAGCTCCTAGTCCAAT-3′ and 5′-TCTTCCGGATTCGAGAAAACGA-3′. The coding sequence of $FMO_{GS\text{-}OX5}$ (*At1g12140*) was amplified with the following primers: 5′-ATGGCACCAGCACGAACCCGA-3′ and 5′-AGATTCCAATAACTGAGAAGGAAG-3′. The amplified PCR products were cloned into pBAD-TOPO vector using pBAD-TOPO TA expression kit (Invitrogen) according to the manufacturer's protocol, resulting in Ara-inducible expression constructs for His-tagged $FMO_{GS\text{-}OX}$ proteins. The constructs were confirmed by sequencing. Constructs expressing $FMO_{GS\text{-}OX}$ proteins and a negative control (empty pBAD-TOPO vector) were transformed into the *E. coli* strain TOP10 (Invitrogen). Expression of $FMO_{GS\text{-}OX}$s was performed according to the manufacturer's recommendation with 0.02% Ara followed by growth at 28°C, 250 rpm for 2 h. *E. coli* spheroplasts were isolated as previously described (Hansen et al., 2007).

Spheroplast Enzymatic Assays

The enzymatic activity of the four $FMO_{GS\text{-}OX}$s was analyzed by spheroplast enzymatic assays. A 100-μL volume of assay solution contained spheroplasts corresponding to 50 μg of total *E. coli* protein, substrate, 0.1 M Tricine (pH 7.9),

and 0.25 mM NADPH. The reaction mixture was incubated for 1 h at 30°C followed by the addition of 100 μL methanol and centrifugation at 5,000*g* for 2 min. Supernatant (200 μL) was lyophilized and dissolved in 50 μL water. In the assays using desulfo 4-MTB GSL as substrate, final substrate concentration was 0.25 mM. In the assays using desulfo GSL extracts from Arabidopsis seeds as substrate, final concentration was 2 mM total GSLs.

Plant Growth

Plants were grown in a growth chamber at a photosynthetic flux of 100 μE at 20°C and 70% relative humidity with a 16/8-h photoperiod.

Genotyping and RT-PCR of *FMO*$_{GS\text{-}OX}$ T-DNA Insertion Mutants

Two T-DNA insertion mutants for each of *FMO*$_{GS\text{-}OX2}$ and *FMO*$_{GS\text{-}OX4}$ and one T-DNA insertion mutant for *FMO*$_{GS\text{-}OX5}$ in Col-0 background were obtained. One T-DNA insertion mutant in ecotype L*er* background was obtained for *FMO*$_{GS\text{-}OX3}$.

The insertion mutants for *FMO*$_{GS\text{-}OX2}$ were the Salk_080561 line (*FMO*$_{GS\text{-}OX2}$-a) and Salk_098896 line (*FMO*$_{GS\text{-}OX2}$-b; Alonso et al., 2003). Primers for genotyping *FMO*$_{GS\text{-}OX2}$-a were 5′-TTTCCCACGATGAGATCTTTG-3′, 5′-TGCGTGTCTTTATAACACGTTTC-3′, and the T-DNA-specific primer LBa1 5′-TGGTTCACGTAGTGGGCCATCG-3′. Primers for genotyping *FMO*$_{GS\text{-}OX2}$-b are 5′-TTTGCCACTGCTGGATTTTAG-3′, 5′-ACCCAGTGCAATACACAATGC-3′, and T-DNA-specific primer LBa1.

The insertion mutant for *FMO*$_{GS\text{-}OX3}$ was GT13906 line (Martienssen, 1998) in L*er* background and genotyping primers were 5′-CCAAGCTTGATTAACTCGCATC-3′, 5′-GCTCTAGACGCAATGTGGACTT-3′, and T-DNA-specific primer DS$_{5\text{-}2}$, 5′-GCGTTTTGTATATCCCGTTTCCGT-3′.

The insertion mutants for *FMO*$_{GS\text{-}OX4}$ were Salk-059185 line (*FMO*$_{GS\text{-}OX4}$-a) and Salk_078861 line (*FMO*$_{GS\text{-}OX4}$-b; Alonso et al., 2003). Genotyping primers for *FMO*$_{GS\text{-}OX4}$-a were 5′-CATTTCGCAGAACCAAACATC-3′, 5′-GACGTTTTTCGAAAGTGTTGG-3′, and T-DNA-specific primer LBa1. Genotyping primers for *FMO*$_{GS\text{-}OX4}$-b were 5′-TAGCGCAGGTGGAAAAATATG-3′, 5′-AACGTTGGGATACGTGTTGAG-3′, and T-DNA-specific primer LBa1.

The insertion mutants for *FMO*$_{GS\text{-}OX5}$ were WiscDsLox361H10 line (Woody et al., 2007). Genotyping primers for *FMO*$_{GS\text{-}OX5}$ were 5′-CCCTGGCCATGAATCTATACC-3′, 5′-AAAATGTCTTCGGTTGGTTCC-3′, and T-DNA-specific primer 5′-AACGTCCGCAATGTGTTATTAAGTTGTC-3′.

Leaves from homozygous *FMO*$_{GS\text{-}OX2}$-a, *FMO*$_{GS\text{-}OX2}$-b, *FMO*$_{GS\text{-}OX3}$, *FMO*$_{GS\text{-}OX4}$-a, *FMO*$_{GS\text{-}OX4}$-b, and *FMO*$_{GS\text{-}OX5}$ were harvested 20 to 25 d after germination. RNA was extracted with TRIzol reagent (Invitrogen) according to the manufacturer's instructions. First-strand cDNA was synthesized using the iScript cDNA synthesis kit (Bio-Rad). The primers used in cloning of each gene for heterologous expression in *E. coli* were used as RT-PCR primers.

GSL Extraction and Analysis

GSL extraction was performed as previously described (Hansen et al., 2007). Fifty to 100 mg leaves and 10 to 20 mg seeds materials were used for the extraction. HPLC analysis was described previously (Hansen et al., 2007).

Analysis of GSL Content in *FMO*$_{GS\text{-}OX}$ Knockout Mutants

For each *FMO*$_{GS\text{-}OX}$ T-DNA insertion mutant line, a single heterozygous plant was allowed to self-pollinate. Plants from segregating seeds were grown in two independent replicates. At 20 to 25 d, individual leaves from each plant were harvested for GSL analysis and for PCR genotyping. GSL contents in wild-type, heterozygous, and homozygous plants were compared. Nested ANOVA was used to test the impact of the T-DNA insertion within each of *FMO*$_{GS\text{-}OX}$ genes on all individual GSLs and resultant variables as described previously (Hansen et al., 2007). Seeds were analyzed the same way as leaves.

FMO$_{GS\text{-}OX}$ Overexpression in Arabidopsis

The coding sequences of the four *FMO*$_{GS\text{-}OX}$s were amplified from the constructs for the heterologous expression in *E. coli* (described above) with Pfu Turbo C$_X$ Hotstart DNA polymerase (Stratagene). The overexpression constructs driven by the cauliflower mosaic virus 35S promoter were created by cloning the above PCR product into pCAMBIA230035Su using the USER method as described (Nour-Eldin et al., 2006).

Primers for amplification of *FMO*$_{GS\text{-}OX2}$ were 5′-GCTTAAUATGGCACCAGCTCAAAACC-3′ and 5′-GGTTTAAUTTAGAGGATATGGGAAGG-3′. Primers for *FMO*$_{GS\text{-}OX3}$ were 5′-GGCTTAAUATGGCACCAGCTCAAAACCA-3′ and 5′-GGTTTAAUCATCTTCCATTTTCGAGGTAATAA-3′.

Primers for *FMO*$_{GS\text{-}OX4}$ were 5′-GGCTTAAUATGGCACCAGCTC-3′ and 5′-GGTTTAAUCGTAGTCAAACTTCATCTTCCG-3′. Primers for *FMO*$_{GS\text{-}OX5}$ were 5′-GGCTTAAUATGGCACCAGCACGAACCCGA-3′ and 5′-GGTTTAAUTCAAGATTCCAATAACTGAGAAGG-3′.

Plant Transformation

The overexpression constructs with *FMO*$_{GS\text{-}OX}$s driven by the 35S promoter were transformed into *Agrobacterium tumefaciens* strain C58 (Zambryski et al., 1983), and then into Arabidopsis (Col-0) via the floral-dip method (Zhang et al., 2006a). Transgenic plants were selected on 0.5× Murashige and Skoog medium with 50 $\mu g \cdot mL^{-1}$ kanamycin.

Analysis of GSL Content in *FMO*$_{GS\text{-}OX}$ Overexpression Lines

For each *FMO*$_{GS\text{-}OX}$ gene, two independent T$_1$ transgenic lines with high FMO$_{GS\text{-}OX}$ activity were selected for further analysis. Plants from each transgenic line were grown in two independent biological replicates. Leaf material from each plant was harvested for GSL analysis and for genotyping for the presence or absence of the *NptII* transgene using the primers 5′-CAGCAATATCACGGGTAGCCA-3′ and 5′-GGCTATTCGGCTATGACTGGG-3′. GSL contents in transgenic and wild-type Arabidopsis plants were compared. Nested ANOVA was used to test the impact of *FMO*$_{GS\text{-}OX}$ overexpression on all individual GSLs and resultant variables as previously described (Hansen et al., 2007). Seeds were harvested and analyzed the same way as described above.

Supplemental Data

The following materials are available in the online version of this article.

Supplemental Figure S1. Confirmation of *FMO*$_{GS\text{-}OX}$ T-DNA mutants by RT-PCR.

Supplemental Figure S2. GSL profile of seed in T$_1$ generation of *35S*::*FMO*$_{GS\text{-}OX4}$ and wild-type plants.

Supplemental Table S1. FMO$_{GS\text{-}OX}$ homologous sequences utilized in Figure 2.

Supplemental Table S2. L*er* × Cvi short-chain aliphatic seed FMO$_{GS\text{-}OX}$ analysis.

Supplemental Table S3. L*er* × Cvi short-chain aliphatic leaf FMO$_{GS\text{-}OX}$ analysis.

Supplemental Table S4. GSL profile of *FMO*$_{GS\text{-}OX}$ T-DNA knockout mutants.

Supplemental Table S5. GSL profiles of *35S*::*FMO*$_{GS\text{-}OX4}$ overexpression lines and wild-type plants.

Supplemental Table S6. Altered FMO$_{GS\text{-}OX}$ activity in the T$_1$ generation of *FMO*$_{GS\text{-}OX4}$ overexpression lines.

Received July 7, 2008; accepted September 14, 2008; published September 17, 2008.

LITERATURE CITED

Alonso JM, Stepanova AN, Leisse TJ, Kim CJ, Chen H, Shinn P, Stevenson DK, Zimmerman J, Barajas P, Cheuk R, et al (2003) Genome-wide insertional mutagenesis of *Arabidopsis thaliana*. Science **301:** 653–657

Blanc G, Wolfe KH (2004) Widespread paleopolyploidy in model plant species inferred from age distributions of duplicate genes. Plant Cell **16:** 1667–1678

Burow M, Zhang ZY, Ober JA, Lambrix VM, Wittstock U, Gershenzon J, Kliebenstein DJ (2008) ESP and ESM1 mediate indol-3-acetonitrile production from indol-3-ylmethyl glucosinolate in Arabidopsis. Phytochemistry **69:** 663–671

Cashman JR, Zhang J (2006) Human flavin-containing monooxygenases. Annu Rev Pharmacol Toxicol **46:** 65–100

Eswaramoorthy S, Bonanno JB, Burley SK, Swaminathan S (2006) Mechanism of action of a flavin-containing monooxygenase. Proc Natl Acad Sci USA **103:** 9832–9837

Fahey JW, Haristoy X, Dolan PM, Kensler TW, Scholtus I, Stephenson KK, Talalay P, Lozniewski A (2002) Sulforaphane inhibits extracellular, intracellular, and antibiotic-resistant strains of Helicobacter pylori and prevents benzo[a]pyrene-induced stomach tumors. Proc Natl Acad Sci USA **99:** 7610–7615

Giamoustaris A, Mithen R (1996) Genetics of aliphatic glucosinolates. IV. Side-chain modification in Brassica oleracea. Theor Appl Genet **93:** 1006–1010

Gu Z, Rifkin SA, White KP, Li WH (2004) Duplicate genes increase gene expression diversity within and between species. Nat Genet **36:** 577–579

Halkier BA, Gershenzon J (2006) Biology and biochemistry of glucosinolates. Annu Rev Plant Biol **57:** 303–333

Hansen BG, Kliebenstein DJ, Halkier BA (2007) Identification of a flavin-monooxygenase as the *S*-oxygenating enzyme in aliphatic glucosinolate biosynthesis in Arabidopsis. Plant J **50:** 902–910

Kliebenstein DJ (2008) A role for gene duplication and natural variation of gene expression in the evolution of metabolism. PLoS ONE **3:** e1838

Kliebenstein DJ, Figuth A, Mitchell-Olds T (2002) Genetic architecture of plastic methyl jasmonate responses in *Arabidopsis thaliana*. Genetics **161:** 1685–1696

Kliebenstein DJ, Gershenzon J, Mitchell-Olds T (2001a) Comparative quantitative trait loci mapping of aliphatic, indolic and benzylic glucosinolate production in *Arabidopsis thaliana* leaves and seeds. Genetics **159:** 359–370

Kliebenstein DJ, Kroymann J, Brown P, Figuth A, Pedersen D, Gershenzon J, Mitchell-Olds T (2001b) Genetic control of natural variation in Arabidopsis glucosinolate accumulation. Plant Physiol **126:** 811–825

Kliebenstein DJ, Lambrix VM, Reichelt M, Gershenzon J, Mitchell-Olds T (2001c) Gene duplication in the diversification of secondary metabolism: tandem 2-oxoglutarate-dependent dioxygenases control glucosinolate biosynthesis in *Arabidopsis*. Plant Cell **13:** 681–693

Krueger SK, Williams DE (2005) Mammalian flavin-containing monooxygenases: structure/function, genetic polymorphisms and role in drug metabolism. Pharmacol Ther **106:** 357–387

Loudet O, Chaillou S, Camilleri C, Bouchez D, Daniel-Vedele F (2002) Bay-0 × Shahdara recombinant inbred line population: a powerful tool for the genetic dissection of complex traits in Arabidopsis. Theor Appl Genet **104:** 1173–1184

Lynch M, Conery JS (2000) The evolutionary fate and consequences of duplicate genes. Science **290:** 1151–1155

Martienssen RA (1998) Functional genomics: probing plant gene function and expression with transposons. Proc Natl Acad Sci USA **95:** 2021–2026

Nour-Eldin HH, Hansen BG, Norholm MHH, Jensen JK, Halkier BA (2006) Advancing uracil-excision based cloning towards an ideal technique for cloning PCR fragments. Nucleic Acids Res **34:** e122

Rizzon C, Ponger L, Gaut BS (2006) Striking similarities in the genomic distribution of tandemly arrayed genes in Arabidopsis and rice. PLoS Comput Biol **2:** e115

Rohr F, Ulrichs C, Mucha-Pelzer T, Mewis I (2006) Variability of aliphatic glucosinolates in Arabidopsis and their influence on insect resistance. Commun Agric Appl Biol Sci **71:** 507–515

Rose P, Faulkner K, Williamson G, Mithen R (2000) 7-Methylsulfinylheptyl and 8-methylsulfinyloctyl isothiocyanates from watercress are potent inducers of phase II enzymes. Carcinogenesis **21:** 1983–1988

Rose P, Huang Q, Ong CN, Whiteman M (2005) Broccoli and watercress suppress matrix metalloproteinase-9 activity and invasiveness of human MDA-MB-231 breast cancer cells. Toxicol Appl Pharmacol **209:** 105–113

Schlaich NL (2007) Flavin-containing monooxygenases in plants: looking beyond detox. Trends Plant Sci **12:** 412–418

Talalay P, Fahey JW, Healy ZR, Wehage SL, Benedict AL, Min C, Dinkova-Kostova AT (2007) Sulforaphane mobilizes cellular defenses that protect skin against damage by UV radiation. Proc Natl Acad Sci USA **104:** 17500–17505

Tierens KFM, Thomma BPHJ, Brouwer M, Schmidt J, Kistner K, Porzel A, Mauch-Mani B, Cammue BPA, Broekaert WF (2001) Study of the role of antimicrobial glucosinolate-derived isothiocyanates in resistance of Arabidopsis to microbial pathogens. Plant Physiol **125:** 1688–1699

Vision TJ, Brown DG, Tanksley SD (2000) The origins of genomic duplications in Arabidopsis. Science **290:** 2114–2117

Wentzell AM, Rowe HC, Hansen BG, Ticconi C, Halkier BA, Kliebenstein DJ (2007) Linking metabolic QTLs with network and cis-eQTLs controlling biosynthetic pathways. PLoS Genet **3:** e162

West MAL, Kim K, Kliebenstein DJ, van Leeuwen H, Michelmore RW, Doerge RW, Clair DA (2007) Global eQTL mapping reveals the complex genetic architecture of transcript-level variation in Arabidopsis. Genetics **175:** 1441–1450

Woody S, Austin-Phillips S, Amasino R, Krysan P (2007) The WiscDsLox T-DNA collection: an arabidopsis community resource generated by using an improved high-throughput T-DNA sequencing pipeline. J Plant Res **120:** 157–165

Zambryski P, Joos H, Genetello C, Leemans J, Vanmontagu M, Schell J (1983) Ti-plasmid vector for the introduction of DNA into plant-cells without alteration of their normal regeneration capacity. EMBO J **2:** 2143–2150

Zhang X, Henriques R, Lin SS, Niu QW, Chua NH (2006a) Agrobacterium-mediated transformation of Arabidopsis thaliana using the floral dip method. Nat Protocols **1:** 641–646

Zhang Y, Talalay P, Cho CG, Posner GH (1992) A major inducer of anticarcinogenic protective enzymes from broccoli: isolation and elucidation of structure. Proc Natl Acad Sci USA **6:** 2399–2403

Zhang Z, Ober JA, Kliebenstein DJ (2006b) The gene controlling the quantitative trait locus EPITHIOSPECIFIER MODIFIER1 alters glucosinolate hydrolysis and insect resistance in *Arabidopsis*. Plant Cell **18:** 1524–1536

Zimmermann P, Hirsch-Hoffmann M, Hennig L, Gruissem W (2004) GENEVESTIGATOR. Arabidopsis microarray database and analysis toolbox. Plant Physiol **136:** 2621–2632